Available online at www.sciencedirect.com
ScienceDirect
Journal of Nuclear Materials 373 (2008) 402–406
journal of nuclear materials
www.elsevier.com/locate/jnucmat

Boron deposition on the graphite tiles of the RFX device studied by secondary ion mass spectrometry

F. Ghezzi [a,*], A. Tolstogouzov [b]

[a] Istituto di Fisica del Plasma (IFP-CNR), Via R. Cozzi 53, 20125 Milano, Italy
[b] Dipartimento di Chimica, Università di Firenze, Via della Lastruccia 3, 50019 Sesto Fiorentino, Italy

Received 25 April 2007; accepted 26 June 2007

Abstract

We report on a systematic surface analysis of the graphite tiles coming from different locations on the first wall of the reversed-field pinch device RFX by secondary ion mass spectrometry. Both boron and the main contaminant species were investigated. The largest values of the total boron intensity are found for tiles positioned in front of the injection valve, the lowest for those at the gap. The in-depth profiles of the normalized boron signals are interpreted as signatures of a plasma–wall interaction, namely of the plasma coming in contact with the wall in restricted regions, mainly determined by the magnetic field configuration, during its lifetime.

PACS: 68.55.Nq

1. Introduction

Wall erosion and re-deposition are major effects of the interaction of a plasma with the surrounding wall, a clue issue in nuclear fusion technology. To keep the radiative losses low, the plasma impurities must be limited to low-Z elements, i.e., the effective charge must approach $Z_{\text{eff}} \cong 1$ as far as possible, which implies that low-Z materials must be used for the first, plasma-facing wall. To this purpose, boronization of the graphite tiles covering the inner wall of the vacuum vessel is adopted in several fusion relevant devices. Another important feature, mostly related to the magnetic field structure, is that the effects of erosion and re-deposition on the tiles are generally expected to be inhomogeneous (localized). Due to this, measurements on a variety of tiles selected from different parts of the vessel wall are required in order for a significant insight in these effects to be achievable. An additional complication comes from the fact that the fusion experiments are carried out in different magnetic configurations, e.g., tokamaks and stellarators, and in vacuum chambers with very different shapes, e.g., with either circular or elongated cross-sections. As a consequence of this each system must be investigated quite individually [1,2] and the general conclusions one can draw are bound to be only qualitative or otherwise to be applicable at best to a limited number of devices.

In this work we report a systematic investigation based on secondary ion mass spectrometry (SIMS) of a series of graphite tiles of the inner wall of reversed-field fusion device RFX after a long exposure to the plasma in the first phase of RFX operation. A point worth being stressed is that during this early phase the dynamic evolution of magneto-hydrodynamic (MHD) perturbations, in particular the so-called tearing modes and plasma disruptions, may have significantly contributed to the plasma–surface interactions.

To reveal the expected correlations between the effects detectable on the tiles and the underlying plasma–wall interactions, SIMS analysis of the tile surfaces and near-surfaces has been performed on a set of tiles coming from

* Corresponding author. Tel.: +39 02 66173209; fax: +39 02 66173239.
E-mail address: ghezzi@ifp.cnr.it (F. Ghezzi).

0022-3115/$ - see front matter
doi:10.1016/j.jnucmat.2007.06.018

different toroidal and poloidal positions in the vacuum vessel of RFX. The main criterion in the selection of the tiles was that of correlating their positions with the known inhomogeneities of the passive stabilizing shell. The major target of our investigation was characterizing the boron distribution in the tiles and its dependence on the poloidal and toroidal coordinates.

2. Tile composition, experimental set-up and measuring procedures

The vacuum vessel of RFX is made of Inconel 625 and the first wall of the device includes 2016 graphite tiles that completely surround the last closed magnetic surface. While basically polycrystalline, the graphite of the tiles, produced by Carbon-Lorraine as PT5890 [3,4], also included amorphous carbon. The boron film was deposited on the tiles via glow discharge cleaning (GDC) in a He atmosphere. The average thickness of the hydrogenated boron film deposited on the tiles has been estimated, over a range of the order of hundred nanometers, using a mechanical profilometer [4]. Extensive investigations of the quality of the boron coatings prior to the exposition to the plasma were performed by a number of groups [5,6] including that of RFX [7,8]. Further, all samples are currently analyzed via Rutherford backscattering [9]. Besides the boron, these analyses reveal the presence of both metallic and non-metallic impurities, such as V, Cr, Mn, Mo, Fe, Co, Ni, Cu, Zn and Se, in almost all the samples.

The samples used in our analysis by the SIMS were cut out from tiles selected from different toroidal rows (A1, A38, A44, A59, A60, A68) and different poloidal positions (T1, T8, T15, T22) (see Fig. 1). The total amount of samples was 24 and their typical size ca. $15 \times 10 \times 1.5\ mm^3$. The SIMS measurements were carried out by a dedicated SIMS set-up based on standard commercial components [10–12]. The equipment was completed by a Hiden EQS 1000 Mass Energy Analyser made of a combination of an electrostatic energy analyser and a quadrupole mass filter. The mass spectra were collected using 6 keV mass-filtered $^{16}O_2^+$ ions generated by a duoplasmatron ion gun (model DP50B by VG Fison). The spectra were produced in sequence, which required no more than 70 s per each. The in-depth elemental distributions were evaluated from the mass spectrometric data just after the end of the related measurements. The primary beam was raster-scanned. The 'crater effect' was avoided by recourse to electronic gating of the registration system. Thanks to this, only secondary ions coming from the limited central area of the crater were collected. The depth of the sputter craters and the surface topography were determined by a Tencor Stylus Profiler P-10. Finally, roughness measurements were also made from three different areas of the samples, each of $600 \times 600\ \mu m^2$ size, randomly chosen on their surfaces. The identification of the ion species in the measured spectra was obtained using the numerical code DECO [13].

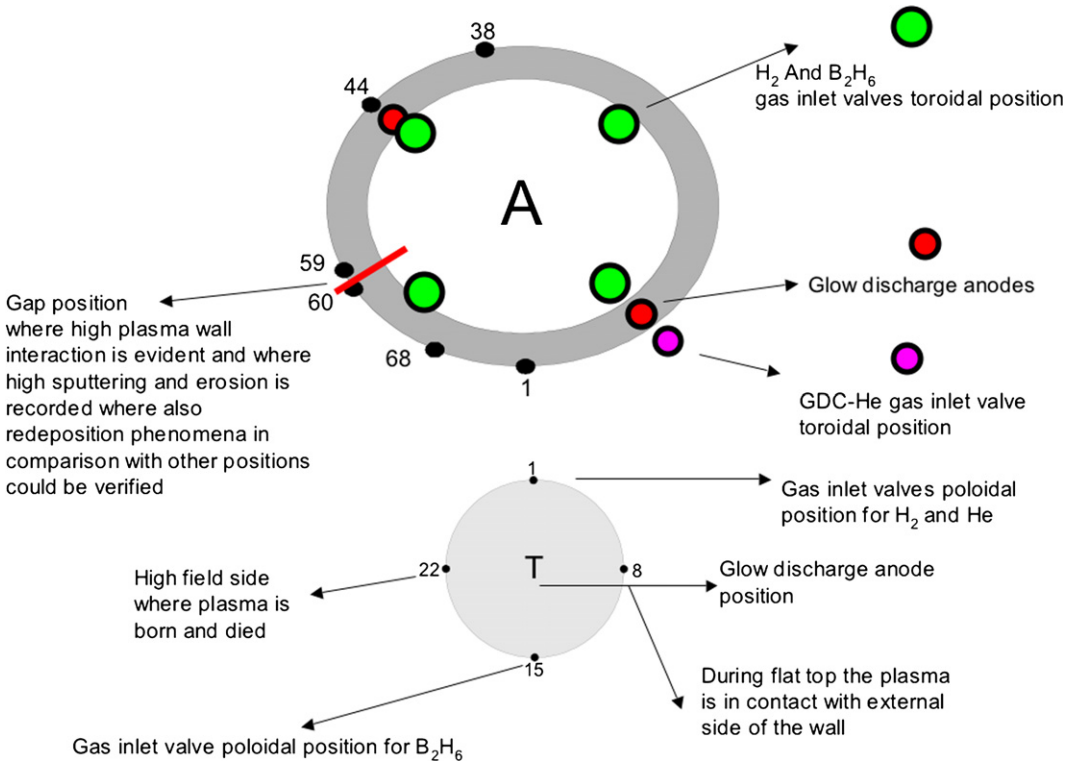

Fig. 1. Schematic view of the sample positions selected for the SIMS measurements (letter A denotes the toroidal rows and letter T the poloidal positions).

3. Experimental results

A typical mass spectrum of the positively charged secondary ions corresponding to a depth of about 1 μm is shown in Fig. 2. The spectrum looks very complex since it includes mass peaks of: (i) atomic ions of the deposited boron and impurities; (ii) surface contaminant species; (iii) oxygen- and hydrogen-containing molecular ions. The distributions of these identified species along the toroidal and poloidal positions have been published elsewhere [14].

Fig. 3 shows the normalized dependences of the $^{10}B^{+}$ signals versus sputtering of the samples from the toroidal row A59. The in-depth boron profiles for the samples coming from other toroidal rows can be found in Ref. [14]. The depth scale in Fig. 3 is derived from the total depth of the sputter crater H as determined by the stylus profilometer

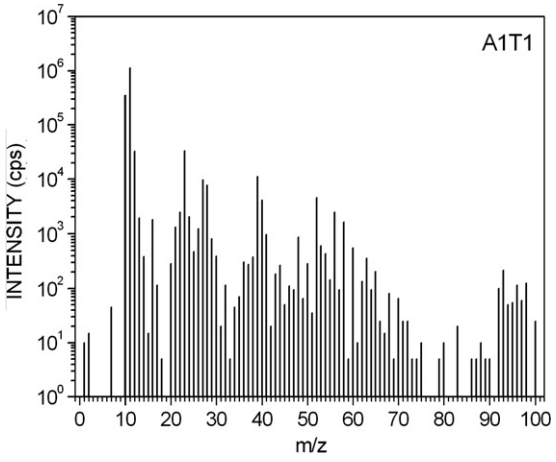

Fig. 2. Mass spectrum of the positive secondary ions measured upon sputtering of the A1–T1 sample. Experimental conditions: $^{16}O_2^{+}$ primary ions, $E_0 = 6$ keV, $I_0 = 250$ nA, raster 0.5×0.5 mm^2, 50% electronic gating.

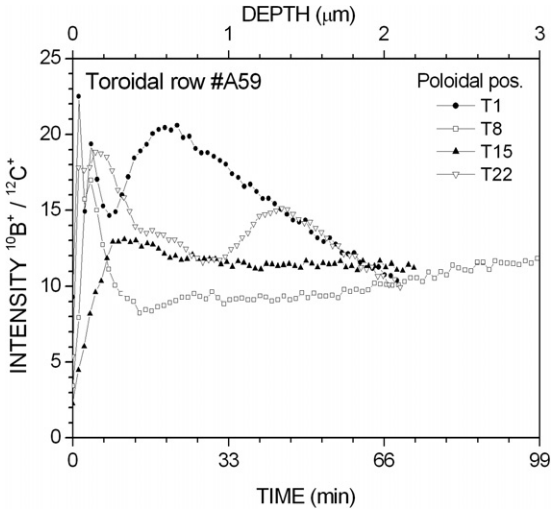

Fig. 3. Normalized boron depth profiles for the samples from the toroidal row A59.

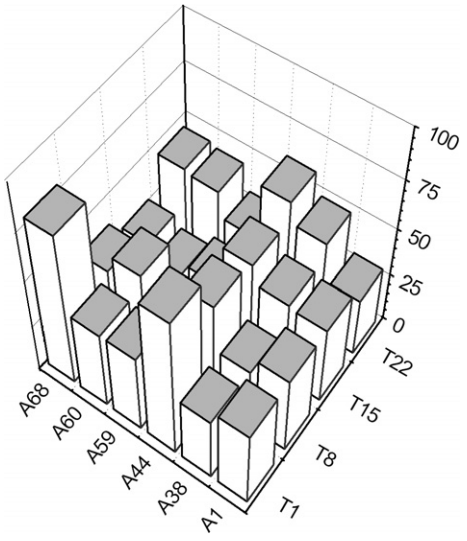

Fig. 4. Intensities of B^{+} ions normalized to the $^{12}C^{+}$ signal and summed up over a depth of 2 μm vs toroidal position at different poloidal sites.

after ending the sputtering. The average erosion rate was assumed to be given by $V_{sp} = dh/dt \cong H/T$, with h the depth sputtered per unit of time, H the total depth sputterd and T the total time of sputtering. The estimated value is $V_{sp} = 30 \pm 15$ nm/min. The trend of the normalized boron intensity summed up within a depth of 2 μm versus the toroidal position at four poloidal sites is shown in Fig. 4.

As regards the identification of the impurity species, the SIMS and XPS (X-ray photoelectron spectroscopy) [15] spectra confirmed both the presence of the metallic and non-metallic elements previously mentioned. In particular, we found that signal levels significantly higher than in all other cases were exhibited: (a) for the toroidal rows A1, A38 and A44 by the samples associated to the poloidal position T15; (b) for the toroidal rows A59, A60 and A68 by the samples associated to the poloidal positions T8 and T22.

4. Discussion of the results

Of special interest are the profiles from row A59 shown in Fig. 3 since their different behavior, namely the fact that the concentrations approach a common value only asymptotically in the depth, can be safely ascribed to deposition for T1 and T22, and to erosion for T8 and T15. This scenario is compatible with a well-known behavior of the plasma, namely with the fact that during the flat top it is in contact with the external wall and then dies on the high-field side. The abrupt changes exhibited by the spectra from surface sub-layers are a result of surface contamination and therefore can be neglected.

Fig. 4 shows that the largest values of the boron signal, more than 75 on our scale in arbitrary units, are found for the samples A44-T1 and A68-T1. As seen in Fig. 1, these tiles were placed near to the H_2 and B_2H_6 gas-inlet valves toroidally and opposite to the same valves poloidally. Also

worth noticing is that the sites with the highest boron concentration do not depend on the distance from the GDC anode. The smallest level of the normalized boron intensity, less than 25, was detected for the samples A59-T8 and A60-T15, and the lowest level for the samples coming from the toroidal row A59. As confirmed also by movies we recorded, the sites indicated in Fig. 1 are effectively those where, on magnetic considerations, the strongest plasma–wall interactions are expected to occur during the high-power discharges. More detailed predictions are difficult to do because, due to the displacement that the plasma column undertakes during its lifetime, the wall surfaces it touches may change in time. The lowest boron concentrations observed for the samples A59-T8 and A60-T15 can be explained as due to their being located just at, and beyond, the gap of the passive stabilizing shell, where the major erosion and re-deposition are generally recorded [16].

The presence of metallic ions (Cr, Mn, Mo, Fe, Co, Ni, Cu) is clearly due to re-deposition of the constituents of the vacuum vessel. The presence of Zn, Se, Zr and V is not very illustrative since it is ascribable to special circumstances. Indeed, the former two elements come from fragments of an optical window imploded during a previous experiment, and the latter two from the electrodes used for edge biasing experiments [9]. As expected, the re-deposition of these elements occurs at the poloidal sites where the magnetic field is higher, i.e., where the plasma either is born or dies. Far from the gap the highest re-deposition occurs at the poloidal position T15. Here too the associated distributions agree with the already quoted displacements of the plasma column.

It is finally worth stressing that some criticality in the interpretation of our results arose due to the roughness of the tile surfaces, due to their long exposure to the plasma (up to 10 000 discharges). Dedicated measurements confirmed that the average roughness of the samples in some cases even exceeded 5 μm, which value is definitely larger than the nominal thickness of the deposited boron layer. Besides this, a substantial distribution of the SIMS depth profiles was produced due to the inhomogeneity of the deposited layers made evident by our SIMS mapping [14].

5. Summary and conclusions

A series of graphite tiles coming from representative and/or critical locations in the vacuum vessel of the RFX device were analyzed by the SIMS technique after a long exposure to the plasma. Both boron and the main contaminant species affecting the tile surfaces were investigated. The selection of the tiles was such as to allow span all the most significant toroidal and poloidal positions. Measurements of the normalized boron intensity in the depth at four poloidal positions and a number of representative toroidal sites were reported. The largest total boron content was found for a tile position practically in front of the injection valve and the lowest near to the gap. The in-depth profiles of the normalized boron signals were unambiguously interpreted as signatures of a wall interaction with the plasma column, as expected. Contaminants from the materials of the vacuum vessel were found all throughout the tiles. The distribution of their surface concentration was found to be in substantial, even if only qualitative, agreement with an interpretation based on the evidence that during its displacements the plasma comes in touch with the wall in preferential regions. Evidence has been also produced that the plasma–wall interaction becomes significantly stronger at the gap of the passive stabilizing shell.

We recognized that the accuracy of our measurements was partially limited by the roughness of the samples, due to their particularly long exposures to the plasma. Adding to the 'natural' imperfections of the surfaces, in same cases the total roughness even exceeded in-depth the nominal thickness of the boron deposited layers. This limiting factor is at a large extent intrinsic to the experimental conditions since, while known, the aging of the tiles normally cannot be chosen at will. Nevertheless in some cases, e.g., in fusion devices with technological mission, one could take profit of the shutdowns of the machine to remove (and replace) the tiles at the most critical sites in order to make them available for periodic measurements in more favorable surface conditions.

As regards the contribution of the MHD activity, namely of the tearing modes and the plasma disruptions, to our data, we can but say that, these effects being likely quite randomly distributed, while possibly affecting the individual measurements, they are not expected to substantially modify the interpretation of our results.

Acknowledgement

We are grateful to P. Sonato (Consorzio RFX, Padua) for fruitful discussions and like to thank C. Pagura (IENI-CNR, Padua) for providing the facilities for the measurements by the SIMS.

References

[1] N. Miya, T. Tanabe, M. Nishikawa, K. Okuno, Y. Hirohata, Y. Oya, J. Nucl. Mater. 329–333 (2004) 74.
[2] G.Y. Sun, M. Friedrich, R. Grötzschel, W. Bürger, R. Behrisch, C. García-Rosales, J. Nucl. Mater. 246 (1997) 9.
[3] Ref. PSP 11 F, Edition 9-81 Le Carbone–Lorraine, Tour Manhattan CEDEX 21, F92095 Paris La Defense 2, France.
[4] F. Gnesotto, P. Sonato, W.R. Baker, A. Doria, F. Elio, M. Fauri, P. Fiorentin, G. Marchiori, G. Zollino, Fusion Eng. Des. 25 (1995) 335.
[5] J. Winter, H.G. Hesser, L. Könen, V. Philipps, H. Reimer, J. Von Seggern, J. Schlüter, E. Wietzke, F. Waelbroeck, P. Wienhold, T. Banno, D. Ringer, S. Veprek, J. Nucl. Mater. 162–164 (1989) 713.
[6] J. Winter, H.G. Hesser, H. Reimer, L. Gobrush, J. Von Seggern, P. Wienhold, J. Nucl. Mater. 176&177 (1990) 486.
[7] P. Sonato, V. Antoni, W.R. Baker, R. Bertoncello, A. Buffa, L. Carraro, S. Costa, G. della Mea, L. Marrelli, A. Murari, M.E. Puiatti, V. Rigato, P. Scarin, L. Tramontin, M. Valisa, S. Zandolin, J. Nucl. Mater. 227 (1996) 259.

[8] L. Tramontin, V. Antoni, M. Bagatin, D. Boscarino, E. Cattaruzza, V. Rigato, S. Zandolin, J. Nucl. Mater. 266–269 (1999) 709.
[9] P. Sonato, private communication.
[10] A. Tolstogouzov, S. Daolio, C. Pagura, Surf. Sci. 441 (1999) 213.
[11] A. Tolstogouzov, S. Daolio, C. Pagura, Nucl. Instrum. Meth. B 183 (2001) 116.
[12] A. Tolstogouzov, S. Daolio, C. Pagura, C.L. Greenwood, Int. J. Mass Spectrom. 214 (2002) 327.
[13] U. Bardi, S. Caporali, S.P. Chenakin, A. Lavacchi, E. Miorin, C. Pagura, A. Tolstogouzov, Surf. Coat. Technol. 209 (2006) 2870.
[14] F. Ghezzi, A. Tolstogouzov, IFP Report FP 07/01, 2007.
[15] F. Ghezzi, M. Sancrotti, F. Dell'Era, IFP Report FP 03/9, 2003.
[16] P. Sonato, V. Antoni, M. Bagatin, W.R. Baker, S. Peruzzo, L. Tramontin, P. Zaccaria, G. Zollino, J. Nucl. Mater. 241–243 (1997) 982.